Editors' Suggestion

SO(5) Non-Fermi Liquid in a Coulomb Box Device

Andrew K. Mitchell,[1,4] Alon Liberman,[2] Eran Sela,[2] and Ian Affleck[3]
[1]*School of Physics, University College Dublin, Belfield, Dublin 4, Ireland*
[2]*School of Physics and Astronomy, Tel Aviv University, Tel Aviv 6997801, Israel*
[3]*Department of Physics and Astronomy and Stewart Blusson Quantum Matter Institute, University of British Columbia, Vancouver, British Columbia V6T 1Z1, Canada*
[4]*Centre for Quantum Engineering, Science, and Technology, University College Dublin, Belfield, Dublin 4, Ireland*

(Received 30 September 2020; accepted 11 March 2021; published 7 April 2021)

Non-Fermi liquid (NFL) physics can be realized in quantum dot devices where competing interactions frustrate the exact screening of dot spin or charge degrees of freedom. We show that a standard nanodevice architecture, involving a dot coupled to both a quantum box and metallic leads, can host an exotic SO(5) symmetry Kondo effect, with entangled dot and box charge and spin. This NFL state is surprisingly robust to breaking channel and spin symmetry, but destabilized by particle-hole asymmetry. By tuning gate voltages, the SO(5) state evolves continuously to a spin and then "flavor" two-channel Kondo state. The expected experimental conductance signatures are highlighted.

DOI: 10.1103/PhysRevLett.126.147702

Nanoelectronic circuit realizations of fundamental quantum impurity models allow the nontrivial physics associated with strong electron correlations to be probed via quantum transport measurements [1]. Quantum dot devices, in particular, can exhibit the Kondo effect at low temperatures [2]: a localized magnetic moment on the dot is dynamically screened by conduction electrons in the metallic leads. Single-dot devices can behave as single-electron transistors, with Kondo-enhanced spin-flip scattering strongly boosting the conductance between source and drain leads measured in experiments [3–5].

The conventional Kondo effect [6] involves a localized "impurity" spin-$\frac{1}{2}$ degree of freedom, coupled to a single effective channel of conduction electrons, and has SU(2) spin symmetry. However, the Kondo effect is also observed in more complex systems, such as coupled quantum dot devices [7,8] and single-molecule transistors [9,10], involving spin and orbital degrees of freedom. In such systems, it is possible to realize variants of the classic spin-$\frac{1}{2}$ single-channel Kondo paradigm: e.g., orbital [11], spin-1 [12,13], and ferromagnetic [14] Kondo effects. In particular, the symmetry of the effective model is important in determining the low-energy physics. Kondo effects with SU(4) symmetry can be realized in double quantum dots [15,16] and carbon nanotube dots [17,18] and also have Fermi liquid (FL) ground states.

More exotic non-Fermi liquid (NFL) states can be realized in multichannel systems, where competing interactions frustrate exact screening of the dot spin or charge degrees of freedom at special high-symmetry points [19]. This results in a residual dot entropy characteristic of fractionalized excitations and anomalous conductance signatures [20,21]. However, this kind of NFL physics is typically delicate, being found at the quantum critical point between more standard FL phases, and is unstable to relevant symmetry-breaking perturbations.

Experimentally, the major challenge to realize NFL Kondo physics in quantum dot devices is to prevent mixing between multiple conduction electron channels. Two prominent scenarios to achieve this utilize an interacting quantum box ("Coulomb box") [22,23]. The quantum box is a large quantum dot, hosting a macroscopically large number of electrons, but due to quantum confinement has a discrete level spacing δ and finite charging energy E_C. For $\delta < T < E_C$ the box effectively provides a continuum reservoir of conduction electrons, but also displays charge quantization [24].

Spin-two channel Kondo (S-2CK) physics can be realized in a device involving a small quantum dot coupled to a

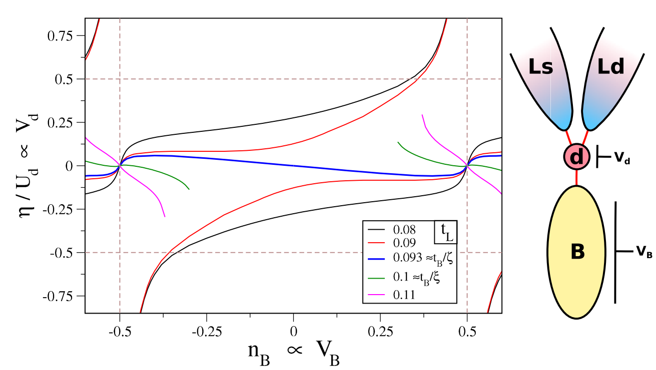

FIG. 1. Right: schematic of the device. A quantum dot coupled to a quantum box and source and drain leads. Left: NRG phase diagram spanned by dot and box gate voltages, $V_d \propto \eta/U_d$ and $V_B \propto n_B$, showing the NFL line for various channel asymmetries t_L/t_B. SO(5) point located at $n_B = \pm\frac{1}{2}$ and $\eta = 0$. Plotted for constant $U_d = 0.3$, $E_C = 0.1$, and $t_B = 0.12$.

quantum box as well as metallic leads [22]. The low-energy effective model consists of a dot spin-$\frac{1}{2}$ exchange coupled to two conduction electron channels (leads and box), with mixing between the channels suppressed by the large box charging energy. Both channels compete to Kondo screen the dot spin, resulting in a NFL state. Breaking channel or spin symmetry relieves the frustration and results in a standard FL state. This physics was realized experimentally in Refs. [25,26].

By contrast, a charge-2CK effect can be realized when a quantum box tuned to its charge degeneracy point is coupled to two leads, as proposed in Ref. [23] and realized experimentally in Refs. [27,28]. In this case, the macroscopic box charge states play the role of a pseudospin impurity. Distinctive signatures of the resulting NFL state are observable in quantum transport [27–34].

In this Letter, we revisit the device of Refs. [22,25,26] but now examine the full phase diagram as function of dot and box gate voltages, which in turn control the dot and box occupancies (see Fig. 1). We show that the emergent SU(4) symmetry of the system arising when the dot hosts a local moment and the box is at its charge degeneracy point is reduced to SO(5) at particle-hole symmetry. Although the SU(4) state is a FL [35], a novel NFL Kondo effect arises at the SO(5) point, in which both dot and box charge and spin are maximally entangled. We achieve a detailed understanding of this state using a combination of conformal field theory [36–38] (CFT), bosonization [39], and numerical renormalization group [40,41] (NRG) techniques. Remarkably, the NFL physics at this point is robust to breaking channel and/or spin symmetry. Furthermore, we show that, by tuning gate voltages, the SO(5) state evolves continuously into the more familiar S-2CK state of Refs. [22,25,26] and then into a flavor-2CK (F-2CK) effect when the dot local moment is lost but box charge fluctuations persist. The distinctive transport signatures associated with this physics are accessible in existing experimental setups.

Models and mappings.—The device illustrated in Fig. 1 is described by the Hamiltonian $H=H_0+H_B+H_d+\sum_\gamma H^\gamma_{\mathrm{hyb}}$, with $\gamma = Ls, Ld, B$ for the source and drain leads and box, respectively. $H_0 = \sum_{\gamma,k,\sigma} \epsilon_{\gamma k} c^\dagger_{\gamma k\sigma} c_{\gamma k\sigma}$ describes the three conduction electron reservoirs, while

$$H_B = E_C(\hat{N}_B - N_0 - n_B)^2, \tag{1}$$

$$H_d = \sum_\sigma \epsilon_d d^\dagger_\sigma d_\sigma + U_d d^\dagger_\uparrow d_\uparrow d^\dagger_\downarrow d_\downarrow \tag{2}$$

describe the box Coulomb interaction and the dot. The dot is tunnel coupled to the leads and box via $H^\gamma_{\mathrm{hyb}} = \sum_{k,\sigma}(t_{\gamma k} d^\dagger_\sigma c_{\gamma k\sigma} + \mathrm{H.c.})$. Here, $\sigma = \uparrow,\downarrow$ denotes (real) spin, and d_σ or $c_{\gamma k\sigma}$ are operators for the dot or conduction electrons, respectively. $\hat{N}_B = \sum_{k,\sigma} c^\dagger_{Bk\sigma} c_{Bk\sigma}$ is the total number operator for the box electrons. The dot and box occupations are controllable by gate voltages $V_d \propto \eta = \epsilon_d + \frac{1}{2} U_d$ and $V_B \propto n_B$, respectively. For simplicity, we now take equivalent conduction electron baths $\epsilon_{\gamma k} \equiv \epsilon_k$ with a constant density of states ν defined inside a band of half-width $D = 1$, such that $\epsilon_k = v_F k$ at low energies. We define $t^2_\gamma = \sum_k |t_{\gamma k}|^2$ and $t^2_L = t^2_{Ls} + t^2_{Ld}$.

Following Ref. [42], we incorporate the box interaction term, Eq. (1), into the hybridization

$$H_B + H^B_{\mathrm{hyb}} \to E_C(\hat{\mathcal{T}}^z - n_B)^2 + \sum_{k,\sigma}(t_{Bk} d^\dagger_\sigma c_{Bk\sigma} \hat{\mathcal{T}}^- + \mathrm{H.c.}),$$

where $\hat{\mathcal{T}}^\pm = \sum_{N_B} |N_B \pm 1\rangle\langle N_B|$ are ladder operators for the box charge, and $\hat{\mathcal{T}}^z = \sum_{N_B}(N_B - N_0)|N_B\rangle\langle N_B|$. Note that the model possesses the symmetry $n_B \to n_B \pm 1$. Particle-hole (PH) asymmetry is controlled by n_B and η; the model is invariant to replacing $n_B \to -n_B$ and $\eta \to -\eta$, related by a PH transformation. Exact PH symmetry arises at $\eta = 0$ for any integer or half-integer n_B.

For the NRG calculations presented here, only a finite number of charge states around the reference N_0 are required to obtain converged results [40,41,43].

Spin-2CK regime.—For large box charging energy E_C and deep in the dot and box Coulomb blockade regime (near the point $\eta = 0$ and $n_B = 0$), the dot hosts an effective spin-$\frac{1}{2}$ local moment, and the box has a well-defined number of electrons N_0. At low temperatures $T \ll E_C, U_d$ virtual charge fluctuations on the dot and box due to H_{hyb} generate the spin-flip scattering responsible for the Kondo effect. However, finite E_C blocks charge transfer between the leads and box, giving rise to a frustration of Kondo screening and the possibility of NFL physics [22]. In this regime, a standard Schrieffer-Wolff transformation (SWT) yields the S-2CK model [19,22]

$$H_{\mathrm{S-2CK}} = H_0 + \vec{S}_d \cdot (\mathcal{J}_L \vec{S}_L + \mathcal{J}_B \vec{S}_B), \tag{3}$$

where $\vec{S}_d$ is a spin-$\frac{1}{2}$ operator for the dot, while $\vec{S}_{\alpha=L,B} = \frac{1}{2}\sum_{\sigma,\sigma'} c^\dagger_{\alpha\sigma} \vec{\boldsymbol{\sigma}}_{\sigma\sigma'} c_{\alpha\sigma'}$, with $c_{B\sigma} = (1/t_B)\sum_k t_{Bk} c_{Bk\sigma}$ and $c_{L\sigma} = (1/t_L)\sum_k (t_{Lsk} c_{Lsk\sigma} + t_{Ldk} c_{Ldk\sigma})$ the local conduction electron orbitals at the dot position, and where

$$\mathcal{J}_L = \frac{8t^2_L}{U_d}\left[1 - \left(\frac{2\eta}{U_d}\right)^2\right]^{-1}; \qquad \mathcal{J}_B = \frac{8t^2_B}{U'_d}\left[1 - \left(\frac{2\eta'}{U'_d}\right)^2\right]^{-1}, \tag{4}$$

with $U'_d = U_d + 2E_C$ and $\eta' = \eta + 2E_C n_B$. Deep in the S-2CK regime, NFL physics arises when $\mathcal{J}_L = \mathcal{J}_B$. For given physical device parameters U_d, E_C, t_L, and t_B, Eq. (4) implies the existence of two NFL *lines* in the (n_B, η) plane related by the symmetry $\eta \to -\eta$ and $n_B \to -n_B$, see Fig. 1. NFL physics can therefore be accessed by tuning the gate voltages $V_d \propto \eta$ and $V_B \propto n_B$, as demonstrated experimentally in this regime in Refs. [25,26]. At the PH symmetric point $\eta = n_B = 0$, S-2CK arises for $t_B = \zeta t_L$ with $\zeta^2 \simeq 1 + 2E_C/U_d$. Although this NFL state is robust to PH asymmetry, it is destabilized by channel asymmetry $\mathcal{J}_L \neq \mathcal{J}_B$ or spin asymmetry $B \neq 0$ [48].

SO(5) Kondo.—At $n_B = \frac{1}{2}$, the box states with N_0 and $(N_0 + 1)$ electrons are exactly degenerate. Neglecting other box charge states (which are $\sim E_C$ higher in energy), we may define charge pseudospin-$\frac{1}{2}$ operators $\hat{T}_B^+ = |N_0 + 1\rangle\langle N_0|$, $\hat{T}_B^- = (\hat{T}_B^+)^\dagger$, and $\hat{T}_B^z = \frac{1}{2}(|N_0 + 1\rangle\langle N_0 + 1| - |N_0\rangle\langle N_0|)$. The charge pseudospin is flipped by electronic tunneling between the dot and box. The low-energy effective model is obtained by projecting onto the dot spin and box pseudospin sectors using a generalized SWT. We now consider explicitly the special point with PH symmetry ($n_B = \frac{1}{2}$ and $\eta = 0$) and channel symmetry ($J_L = J_B \equiv J$, which implies $t_B = \xi t_L$ with $\xi^2 \simeq 1 + 2E_C/U'_d$), whence [49,50]

$$H_{\text{eff}} = H_0 + J\vec{S}_d \cdot \left(c^\dagger_{\alpha\sigma} \frac{\vec{\boldsymbol{\sigma}}_{\sigma\sigma'}}{2} c_{\alpha\sigma'}\right) + V_z \hat{T}_B^z \left(c^\dagger_{\alpha\sigma} \frac{\boldsymbol{\tau}^z_{\alpha\beta}}{2} c_{\beta\sigma}\right) + Q_\perp \vec{S}_d \cdot [c^\dagger_{\alpha\sigma} \vec{\boldsymbol{\sigma}}_{\sigma\sigma'} (\boldsymbol{\tau}^+_{\alpha\beta} \hat{T}_B^- + \boldsymbol{\tau}^-_{\alpha\beta} \hat{T}_B^+) c_{\beta\sigma'}], \tag{5}$$

where the Pauli matrices $\boldsymbol{\sigma}^a$ ($\boldsymbol{\tau}^b$) act in spin (channel) space, and a sum over repeated indices is now implied.

Although initially the coupling constants in Eq. (5) take different values, perturbative scaling [51] shows that the model develops an emergent symmetry $J = V_z = Q_\perp$ at an isotropic low-temperature fixed point. Then the renormalization group (RG) equations reduce to $dJ/dl = 3J^2$, and we have a Kondo scale $T_K^{\text{SO}(5)} \sim D \exp(-1/3\nu J)$.

The fixed point has an unusual SO(5) symmetry, which can be seen by writing Eq. (5) in the symmetric form

$$H_{\text{SO}(5)} = H_0 + J \sum_{A=1}^{10} J^A M^A, \tag{6}$$

where $J^A = c^\dagger_{\alpha\sigma} T^A_{\alpha\beta\sigma\sigma'} c_{\beta\sigma'}$ and $M^A = f^\dagger_{\alpha\sigma} T^A_{\alpha\beta\sigma\sigma'} f_{\beta\sigma'}$ in terms of a fermionic impurity operator carrying both flavor and spin labels subject to the constraint $f^\dagger_{\alpha\sigma} f_{\alpha\sigma} = 1$ such that $\hat{S}^a_d = \frac{1}{2} f^\dagger_{\alpha\sigma} \boldsymbol{\sigma}^a_{\sigma\sigma'} f_{\alpha\sigma'}$ and $\hat{T}^b_B = \frac{1}{2} f^\dagger_{\alpha\sigma} \boldsymbol{\tau}^b_{\alpha\beta} f_{\beta\sigma}$. Here, $\{T^A\}$ are the ten generators of SO(5) [52], $T^{ab} = -T^{ba}$ (with $a, b = 1, \ldots, 5$) satisfying the algebra $[T^{ab}, T^{cd}] = -i(\delta_{bc} T^{ad} - \delta_{ac} T^{bd} - \delta_{bd} T^{ac} + \delta_{ad} T^{bc})$ in the four-dimensional spinor representation

$$\frac{1}{2}\sigma^{a=1,2,3}\tau^1 = T^{a4}, \qquad \frac{1}{2}\sigma^1\tau^0 = T^{23}, \qquad \frac{1}{2}\sigma^3\tau^0 = T^{12},$$
$$\frac{1}{2}\sigma^{a=1,2,3}\tau^2 = T^{a5}, \qquad \frac{1}{2}\sigma^2\tau^0 = T^{31}, \qquad \frac{1}{2}\sigma^0\tau^3 = T^{45},$$

establishing the equivalence between Eqs. (5) and (6).

We applied the machinery of CFT [36–38] to analyze the fixed point properties using the symmetry decomposition $\text{U}(1)_c \times Z_2 \times \text{SO}(5)_1$. Here, U(1) corresponds to the charge sector and Z_2 is an Ising model. The primary fields of the $\text{SO}(5)_1$ theory consist of a singlet with scaling dimension 0, a spinor with scaling dimension $\frac{5}{16}$, and a vector with scaling dimension $\frac{1}{2}$ [53]. The SO(5) fixed point can be obtained by fusion with the spinor under which the impurity transforms.

The finite size spectrum provides a means of characterizing the fixed point. For an effective 1D system of length L, the energies (E) in units of $2\pi v_F/L$, and corresponding degeneracies (No.), can be determined from CFT. We find [43] $(E, \text{No.}) = (0,2), (\frac{1}{8},4), (\frac{1}{2},10), (\frac{5}{8},12), (1,26), \ldots$, consistent with our NRG results and establishing the new SO(5) fixed point as NFL. Interestingly, this spectrum is identical to that of the standard S-2CK model [37]. The entropy at the fixed point is given in terms of the modular S-matrix within CFT [36–38], and here yields $S_{\text{imp}} = \frac{1}{2}\ln(2)$, consistent with NRG [Fig. 2(a)], again reminiscent of S-2CK.

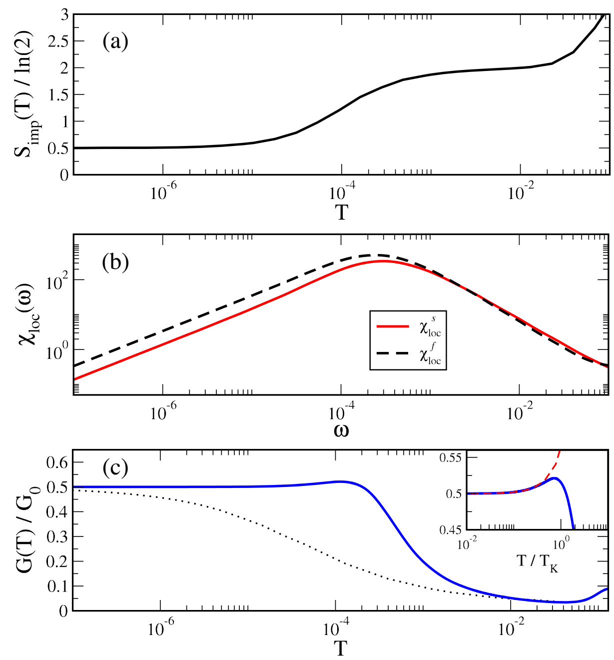

FIG. 2. Physical properties of the SO(5) Kondo effect, obtained by NRG for $n_B = \frac{1}{2}$, $\eta = 0$, $U_d = 0.3$, $E_C = 0.1$, $t_L = 0.085$, and $t_B \simeq \xi t_L = 0.1$. (a) Impurity contribution to entropy $S_{\text{imp}}(T)$, showing partial quenching of the entangled spin and flavor degrees of freedom on the scale of the Kondo temperature $T_K \sim 10^{-4}$. For $T_K \ll T \ll E_C$, free impurity spin and flavor give a ln(4) entropy, while $S_{\text{imp}}(T) = \frac{1}{2}\ln(2)$ for $T \ll T_K$, characteristic of the free Majorana fermion at the SO(5) fixed point. (b) $T = 0$ local spin and flavor dynamical susceptibilities, both showing apparent FL-like behavior $\chi_{\text{loc}}(\omega) \sim \omega$ for $\omega \ll T_K$. (c) Linear response conductance through the dot $G(T)/G_0$ (blue line), with $G = \frac{1}{2}G_0$ at $T = 0$, and leading behavior $G(T) - G(0) \sim +(T/T_K)^{3/2} G_0$ (inset, dashed line). The standard spin-2CK conductance line shape is given for comparison as the dotted line.

However, differences from the standard S-2CK picture can be seen in dynamical quantities such as the local susceptibilities and conductance—see Figs. 2(c) and 2(d). Since the impurity spin $\vec{S}$ and pseudospin $\vec{T}$ operators are absorbed into the conduction electrons at the strong coupling fixed point, they must transform among the ten generators of SO(5). But such fields occur only as *descendants* in $\mathrm{SO}(5)_1$, and so spin-spin correlation functions appear FL-like, $\chi^s_{\mathrm{loc}}(\omega) \sim \omega$ (similar for flavor susceptibility). This contrasts to the regular k-channel Kondo effect: the spin $\mathrm{SU}(2)_k$ theory contains a vector field that transforms as the three components of the impurity spin, with scaling dimension $[2/(2+k)]$, which leads to anomalous NFL properties in the spin susceptibility $\chi^s_{\mathrm{loc}} \sim \omega^{-(k-2/k+2)}$. The SO(5) point appears to have been missed in Ref. [49] because of the apparent FL scaling of its susceptibilities. However, the $\frac{1}{2}\ln(2)$ residual entropy is a clear NFL signature. Furthermore, we find a nonmonotonic conductance, with a NFL leading power law $G(T) - G(0) \sim +T^{3/2}$. This contrasts to S-2CK conductance, which approaches its fixed point value as $-\sqrt{T}$ [22,54–56] or $-T^2$ FL conductance for 1CK [2].

To gain further insight, we expand on the bosonization and refermionization techniques [57] developed by Emery and Kivelson (EK) for the S-2CK model [39] and include the coupling to the flavor degree of freedom. This method allows us to express a spin and flavor anisotropic version of Eq. (5) in terms of local fermions $d \propto S^-_d$ and $a \propto T^-_B$, relating to impurity spin and flavor degrees of freedom, with corresponding Majorana operators $d_+ = (1/\sqrt{2})(d^\dagger + d)$ and $d_- = (1/\sqrt{2}i)(d^\dagger - d)$, and similar for a, as well as a 1D bulk fermionic "spin-flavor" field for the conduction electrons denoted $\psi_{sf}(x)$, with Majorana components $\chi_+ = (1/\sqrt{2})[\psi^\dagger_{\mathrm{sf}}(0) + \psi_{\mathrm{sf}}(0)]$, $\chi_- = (1/\sqrt{2}i)[\psi^\dagger_{\mathrm{sf}}(0) - \psi_{\mathrm{sf}}(0)]$. The resulting EK Hamiltonian takes the simple quadratic form [43]

$$H_{\mathrm{EK}} = H_0 + iJ_\perp d_- \chi_+ - 2iQ_\perp d_+ a_-. \tag{7}$$

The $J_\perp$ term is the usual EK form of the S-2CK interaction. The spin-flavor coupling term $Q_\perp$ couples and gaps out the pair d_+ and a_-. Unlike in the S-2CK model, where d_+ remains decoupled, here we see that it is a_+ that is free at the SO(5) fixed point and is responsible for the $\frac{1}{2}\ln(2)$ residual entropy. The fixed point properties of Eq. (7) describe the physical quantum dot system because the artificial spin-flavor anisotropies used to obtain it are RG irrelevant.

Stability of SO(5) Kondo.—We consider the effect of symmetry-breaking perturbations at the SO(5) point.

Channel asymmetry, corresponding to $t_B \neq \xi t_L$ in the bare model, generates an extra term in Eq. (5) given by $\delta H_{\mathrm{ch}} = J_- \vec{S}_d \cdot (c^\dagger_{\alpha\sigma} \vec{\sigma}_{\sigma\sigma'} \boldsymbol{\tau}^z_{\alpha\beta} c_{\beta\sigma'})$ with $J_- \propto J_B - J_L$. Under the EK mapping, this becomes $\delta H_{\mathrm{ch}} = -iJ_- d_+ \chi_-$ as in the S-2CK model. But in contrast to the S-2CK model, the SO(5) point is not destabilized by this perturbation because the d_+ Majorana involved in J_- is already gapped out by the spin-flavor coupling $Q_\perp$ in Eq. (7). The a_+ Majorana remains free. Breaking spin symmetry by applying a dot magnetic field $\delta H_s = B\hat{S}^z_d = -iBd_+d_-$ is similarly irrelevant at the SO(5) fixed point. The NFL physics is therefore robust to breaking channel and spin symmetries. This is directly confirmed by NRG [43].

PH symmetry is broken by $\eta \neq 0$ for $n_B = \frac{1}{2}$. Performing the SWT yields an additional contribution to Eq. (5) of the form [50] $\delta H_{\mathrm{PH}} = \frac{1}{2} V_\perp \sum_{b=1,2} \hat{T}^b_B (c^\dagger_{\alpha\sigma} \boldsymbol{\tau}^b_{\alpha\beta} c_{\beta\sigma}) + Q_z \sum_{a=1,2,3} \hat{S}^a_d \hat{T}^3_B (c^\dagger_{\alpha\sigma} \boldsymbol{\sigma}^a_{\sigma\sigma'} \boldsymbol{\tau}^3_{\alpha\beta} c_{\beta\sigma'})$ where $V_\perp, Q_z \propto \eta$. This perturbation contains an additional five generators, which together with the ten from SO(5) form the defining representation of SU(4). Indeed, under RG, the system flows to a fully isotropic SU(4) FL fixed point, as discussed in Refs. [16,35,49], with zero residual entropy. Breaking PH symmetry therefore destabilizes the NFL SO(5) fixed point, with an emergent FL crossover scale $T^* \sim \eta^2$ [43]. Unusually then, lowering the symmetry of the bare model by introducing finite η leads to a low-energy SU(4) fixed point with higher symmetry than the SO(5) fixed point obtained at $\eta = 0$. Applying the EK mapping, we obtain [43] $\delta H_{\mathrm{PH}} = -iV_\perp a_+ \chi_-$. This is a RG relevant term with scaling dimension $\frac{1}{2}$: the previously free a_+ Majorana is now coupled to the χ_- field, quenching the $\frac{1}{2}\ln(2)$ entropy and leading to a FL state, with $\chi^{s,f}_{\mathrm{loc}} \sim \omega$ and $G(T) - G(0) \sim T^2$ [58].

Full phase diagram.—We now explore the entire (n_B,η) plane using NRG, focusing on the quantum critical lines along which NFL physics can be realized in experiment (see Fig. 1). In practice, we tune η for a given n_B to find the critical point, which we identify in NRG from its characteristic $\frac{1}{2}\ln(2)$ residual entropy.

An effective flavor field is generated on moving away from $n_B = \frac{1}{2}$. The resulting perturbation $\delta H_f = B_f \hat{T}^z_B$, with $B_f = E_C(1 - 2n_B)$, breaks PH symmetry and is therefore RG relevant at the SO(5) fixed point. However, the two sources of PH asymmetry from $\eta \neq 0$ and $n_B \neq \frac{1}{2}$ can cancel out [close to the SO(5) point this arises along the line $2Q_\perp V_\perp = J_- B_f$ [58]]. NRG results confirm the continuous evolution of the NFL state on moving from $n_B = \frac{1}{2}$ into the box Coulomb blockade regime centered on $n_B = 0$. In particular, the spin and flavor susceptibilities along the NFL lines in Fig. 3 show the crossover from spin-flavor Kondo to S-2CK.

The NFL line with $t_B/t_L = \zeta$ (blue line, Fig. 1) is invariant to the PH transformation, $n_B \to -n_B$ and $\eta \to -\eta$, and smoothly connects spin-flavor Kondo at all half-odd-integer n_B with S-2CK at all integer n_B. For $t_B/t_L < \zeta$ (green and pink lines, Fig. 1), the NFL lines

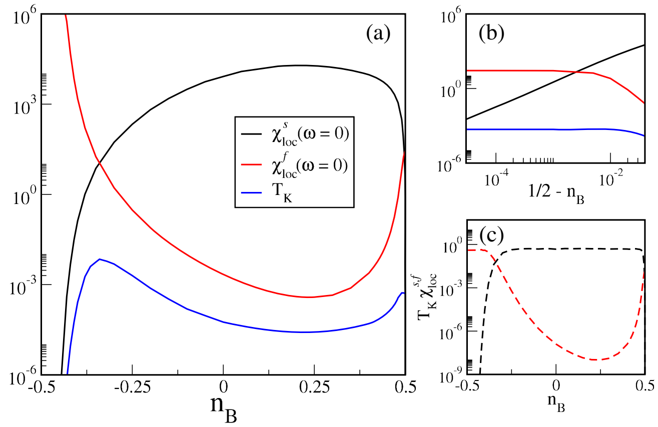

FIG. 3. Evolution along the black NFL line in Fig. 1. (a) $T = \omega = 0$ susceptibilities χ^s_{loc} (black), χ^f_{loc} (red), and Kondo temperature T_K (blue). Flavor fluctuations are suppressed in the box Coulomb blockade regime, while spin fluctuations are suppressed as the dot local moment is lost for $n_B \to -\frac{1}{2}$. (b) Behavior near $n_B = \frac{1}{2}$ showing $\chi^s_{\mathrm{loc}}(0) \sim (\frac{1}{2} - n_B)^2$ [consistent with $\chi^s_{\mathrm{loc}}(\omega) \sim \omega$], while χ^f_{loc} remains finite. (c) $T_K \chi^s_{\mathrm{loc}}$ (black dashed) and $T_K \chi^f_{\mathrm{loc}}$ (red dashed) showing crossover from spin-flavor to S-2CK to F-2CK as n_B is varied from $+\frac{1}{2}$ to $-\frac{1}{2}$.

terminate, signaling that the effective PH asymmetry from n_B can no longer be compensated by tuning η.

By contrast, for $t_B/t_L > \zeta$ (red and black lines, Fig. 1), the NFL lines continue into an unexpected region of the phase diagram where $|\eta|/U_d > \frac{1}{2}$. Here spin fluctuations are suppressed since the dot no longer hosts a local moment, but flavor fluctuations are enhanced (see Fig. 3). The NFL lines in this regime diverge with $\eta \to \pm\infty$ as $n_B \to \pm\frac{1}{2}$, and F-2CK dominates. Along the crossover from S-2CK to F-2CK, spin and flavor fluctuations become equally balanced at the dot charge degeneracy point $|\eta| = \frac{1}{2} U_d$. The NFL state at this point develops at a strongly enhanced Kondo temperature (Fig. 3), making it particularly well suited to experimental investigation.

Conclusions.—We revisit a classic model describing coupled quantum dot and box devices used in experiments to probe NFL physics, uncovering a rich range of new physics, including a novel spin-flavor SO(5) Kondo effect. We study the evolution of the NFL line as a function of dot and box gate voltages using a combination of analytical and numerical techniques, showing that the well-known S-2CK effect can continuously transform into the F-2CK or SO(5) Kondo effects. Distinctive experimental signatures of this new physics should be observable in conductance [58].

We thank Josh Folk for stimulating discussions. A. K. M. and E. S. thank the Stewart Blusson Quantum Matter Institute (UBC) for travel support. A. K. M. acknowledges funding from the Irish Research Council Laureate Awards 2017/2018 through Grant No. IRCLA/2017/169. E. S. acknowledges support from ARO (W911NF-20-1-0013), the Israel Science Foundation Grant No. 154/19 and U.S.-Israel Binational Science Foundation (Grant No. 2016255). I. A. acknowledges support from NSERC Discovery Grant No. 04033-2016.

[1] L. L. Sohn, L. P. Kouwenhoven, and G. Schön, *Mesoscopic Electron Transport* (Springer Science & Business Media, New York, 2013), Vol. 345.
[2] M. Pustilnik and L. Glazman, J. Phys. Condens. Matter **16**, R513 (2004).
[3] D. Goldhaber-Gordon, H. Shtrikman, D. Mahalu, D. Abusch-Magder, U. Meirav, and M. Kastner, Nature (London) **391**, 156 (1998).
[4] S. M. Cronenwett, T. H. Oosterkamp, and L. P. Kouwenhoven, Science **281**, 540 (1998).
[5] W. Van der Wiel, S. De Franceschi, T. Fujisawa, J. Elzerman, S. Tarucha, and L. Kouwenhoven, Science **289**, 2105 (2000).
[6] A. C. Hewson, *The Kondo Problem to Heavy Fermions* (Cambridge University Press, Cambridge, England, 1997).
[7] H. Jeong, A. M. Chang, and M. R. Melloch, Science **293**, 2221 (2001).
[8] J. Malecki, E. Sela, and I. Affleck, Phys. Rev. B **82**, 205327 (2010).
[9] W. Liang, M. P. Shores, M. Bockrath, J. R. Long, and H. Park, Nature (London) **417**, 725 (2002).
[10] A. K. Mitchell, K. G. Pedersen, P. Hedegård, and J. Paaske, Nat. Commun. **8**, 1 (2017).
[11] R. López, D. Sánchez, M. Lee, M.-S. Choi, P. Simon, and K. Le Hur, Phys. Rev. B **71**, 115312 (2005).
[12] S. Sasaki, S. De Franceschi, J. Elzerman, W. Van der Wiel, M. Eto, S. Tarucha, and L. Kouwenhoven, Nature (London) **405**, 764 (2000).
[13] J. Paaske, A. Rosch, P. Wölfle, N. Mason, C. Marcus, and J. Nygård, Nat. Phys. **2**, 460 (2006).
[14] A. K. Mitchell, T. F. Jarrold, and D. E. Logan, Phys. Rev. B **79**, 085124 (2009).
[15] A. Keller, S. Amasha, I. Weymann, C. Moca, I. Rau, J. Katine, H. Shtrikman, G. Zaránd, and D. Goldhaber-Gordon, Nat. Phys. **10**, 145 (2014).
[16] L. Borda, G. Zaránd, W. Hofstetter, B. I. Halperin, and J. von Delft, Phys. Rev. Lett. **90**, 026602 (2003); M. R. Galpin, D. E. Logan, and H. R. Krishnamurthy, Phys. Rev. Lett. **94**, 186406 (2005).
[17] M.-S. Choi, R. López, and R. Aguado, Phys. Rev. Lett. **95**, 067204 (2005).
[18] F. B. Anders, D. E. Logan, M. R. Galpin, and G. Finkelstein, Phys. Rev. Lett. **100**, 086809 (2008).
[19] P. Nozieres and A. Blandin, J. Phys. **41**, 193 (1980).
[20] I. Affleck and A. W. W. Ludwig, Phys. Rev. Lett. **67**, 161 (1991).
[21] I. Affleck and A. W. W. Ludwig, Phys. Rev. B **48**, 7297 (1993).
[22] Y. Oreg and D. Goldhaber-Gordon, Phys. Rev. Lett. **90**, 136602 (2003).
[23] A. Furusaki and K. A. Matveev, Phys. Rev. B **52**, 16676 (1995).
[24] K. A. Matveev, Phys. Rev. B **51**, 1743 (1995).
[25] R. Potok, I. Rau, H. Shtrikman, Y. Oreg, and D. Goldhaber-Gordon, Nature (London) **446**, 167 (2007).

[26] A. Keller, L. Peeters, C. Moca, I. Weymann, D. Mahalu, V. Umansky, G. Zaránd, and D. Goldhaber-Gordon, Nature (London) **526**, 237 (2015).

[27] Z. Iftikhar, S. Jezouin, A. Anthore, U. Gennser, F. Parmentier, A. Cavanna, and F. Pierre, Nature (London) **526**, 233 (2015).

[28] Z. Iftikhar, A. Anthore, A. Mitchell, F. Parmentier, U. Gennser, A. Ouerghi, A. Cavanna, C. Mora, P. Simon, and F. Pierre, Science **360**, 1315 (2018).

[29] A. K. Mitchell, L. A. Landau, L. Fritz, and E. Sela, Phys. Rev. Lett. **116**, 157202 (2016).

[30] L. A. Landau, E. Cornfeld, and E. Sela, Phys. Rev. Lett. **120**, 186801 (2018).

[31] T. K. T. Nguyen and M. N. Kiselev, Phys. Rev. Lett. **125**, 026801 (2020).

[32] D. B. Karki and M. N. Kiselev, Phys. Rev. B **102**, 241402(R) (2020).

[33] G. A. R. van Dalum, A. K. Mitchell, and L. Fritz, Phys. Rev. B **102**, 041111(R) (2020); **102**, 205137 (2020).

[34] June-Young M. Lee, C. Han, and H.-S. Sim, Phys. Rev. Lett. **125**, 196802 (2020).

[35] K. Le Hur and P. Simon, Phys. Rev. B **67**, 201308(R) (2003).

[36] I. Affleck, Nucl. Phys. **B336**, 517 (1990).

[37] I. Affleck and A. W. Ludwig, Nucl. Phys. **B360**, 641 (1991).

[38] I. Affleck, Acta Phys. Pol. B **26**, 1869 (1995).

[39] V. J. Emery and S. Kivelson, Phys. Rev. B **46**, 10812 (1992).

[40] K. G. Wilson, Rev. Mod. Phys. **47**, 773 (1975); R. Bulla, T. A. Costi, and T. Pruschke, Rev. Mod. Phys. **80**, 395 (2008).

[41] A. K. Mitchell, M. R. Galpin, S. Wilson-Fletcher, D. E. Logan, and R. Bulla, Phys. Rev. B **89**, 121105(R) (2014); K. M. Stadler, A. K. Mitchell, J. von Delft, and A. Weichselbaum, Phys. Rev. B **93**, 235101 (2016).

[42] F. B. Anders, E. Lebanon, and A. Schiller, Phys. Rev. B **70**, 201306(R) (2004).

[43] See Supplemental Material at http://link.aps.org/supplemental/10.1103/PhysRevLett.126.147702 for (i) additional NRG data, (ii) details of NRG and conductance calculations, and (iii) further information on the CFT treatment and Emery-Kivelson mapping. Additional references [44–47] are contained therein.

[44] A. Weichselbaum and J. von Delft, Phys. Rev. Lett. **99**, 076402 (2007).

[45] Y. Meir and N. S. Wingreen, Phys. Rev. Lett. **68**, 2512 (1992).

[46] A. K. Mitchell, E. Sela, and D. E. Logan, Phys. Rev. Lett. **108**, 086405 (2012).

[47] J. Ye, Phys. Rev. B **56**, R489 (1997).

[48] I. Affleck, A. W. W. Ludwig, H.-B. Pang, and D. L. Cox, Phys. Rev. B **45**, 7918 (1992).

[49] K. Le Hur, P. Simon, and L. Borda, Phys. Rev. B **69**, 045326 (2004).

[50] See Eq. (17) in Ref. [49].

[51] See Eq. (20) in Ref. [49] with $V_{\perp} = Q_z = 0$.

[52] H. Georgi, *Lie Algebras in Particle Physics: From Isospin to Unified Theories* (CRC Press, Boca Raton, FL, 2018).

[53] P. Francesco, P. Mathieu, and D. Sénéchal, *Conformal Field Theory* (Springer Science & Business Media, New York, 2012).

[54] M. Pustilnik, L. Borda, L. I. Glazman, and J. von Delft, Phys. Rev. B **69**, 115316 (2004).

[55] E. Sela, A. K. Mitchell, and L. Fritz, Phys. Rev. Lett. **106**, 147202 (2011).

[56] A. K. Mitchell and E. Sela, Phys. Rev. B **85**, 235127 (2012).

[57] J. Von Delft and H. Schoeller, Ann. Phys. (Berlin) **7**, 225 (1998).

[58] A. Liberman, A. K. Mitchell, I. Affleck, and E. Sela, arXiv:2103.10680.